

# SCIENTIFIC REPORTS



OPEN

## Metagenomic insight into the microbial networks and metabolic mechanism in anaerobic digesters for food waste by incorporating activated carbon

Jingxin Zhang<sup>1</sup>, Liwei Mao<sup>2</sup>, Le Zhang<sup>2</sup>, Kai-Chee Loh<sup>2</sup>, Yanjun Dai<sup>3</sup> & Yen Wah Tong<sup>1,2</sup> 

Powdered activated carbon (AC) is commonly used as an effective additive to enhance anaerobic digestion (AD), but little is known about how the metabolic pathways resulting from adding AC change the microbial association network and enhance food waste treatment. In this work, the use of AC in an anaerobic digestion system for food waste was explored. Using bioinformatics analysis, taxonomic trees and the KEGG pathway analysis, changes in microbial network and biometabolic pathways were tracked. The overall effect of these changes were used to explain and validate improved digestion performance. The results showed that AC accelerated the decomposition of edible oil in food waste, enhancing the conversion of food waste to methane with the optimized dosage of 12 g AC per reactor. Specifically, when AC was added, the propionate metabolic pathway that converts propanoic acid to acetic acid became more prominent, as measured by 16S rRNA in the microbial community. The other two metabolic pathways, Lipid Metabolism and Methane Metabolism, were also enhanced. Bioinformatics analysis revealed that AC promoted the proliferation of syntrophic microorganisms such as *Methanosaeta* and *Geobacter*, forming a highly intensive syntrophic microbial network.

The increasing food waste (FW) generation around the world has increased the demand for reduction and effective utilization of FW in recent years<sup>1</sup>. The uncontrolled disposal of FW is liable to create public health concerns and cause adverse environmental impacts. Anaerobic digestion (AD) has become a proven and promising approach for FW treatment and bioenergy production<sup>2,3</sup>. During AD process, biodegradable organic matters can be converted into biogas (CH<sub>4</sub> and CO<sub>2</sub>) via anaerobic microorganisms. However, AD of FW still faces challenges in process stability and effectiveness under high organic loading rates (OLRs) during AD process<sup>4</sup>.

AD is a complex biological process, which contains many different consortia of microorganisms with different functions<sup>5</sup>. Specifically, hydrolyzing and fermenting bacteria initially convert complex organic compounds into volatile fatty acids (VFA), alcohols and lactate. These intermediate products are further converted by fermentative bacteria to acetate, H<sub>2</sub>, CO<sub>2</sub>, and formate that are used by methanogens for acetoclastic and hydrogenotrophic methanogenesis. Traditional H<sub>2</sub>-utilizing methanogens can generate methane by using fermentative end-products such as H<sub>2</sub>/CO<sub>2</sub> deriving from the syntrophic metabolism of syntrophic bacteria. The relationship between syntrophic bacteria and H<sub>2</sub>-utilizing methanogens is syntrophic and this process is well-documented interspecies hydrogen transfer (IHT)<sup>6</sup>. The activity of syntrophic bacteria is liable to be affected by the hydrogen concentration in the liquid phase of AD<sup>7</sup>. Under high OLRs, if the removing rate of hydrogen by methanogens is relatively low, the thermodynamics of IHT process will be inhibited, resulting in the accumulation of VFA, pH decline and failure of AD operation.

<sup>1</sup>Environmental Research Institute, National University of Singapore, 1 Create Way, Singapore, 138602, Singapore.

<sup>2</sup>Department of Chemical & Biomolecular Engineering, National University of Singapore, 4 Engineering Drive 4, Singapore, 117576, Singapore. <sup>3</sup>School of Mechanical Engineering, Shanghai Jiao Tong University, 800 Dong Chuan Road, Shanghai, 200240, China. Correspondence and requests for materials should be addressed to Y.W.T. (email: [chetyw@nus.edu.sg](mailto:chetyw@nus.edu.sg))

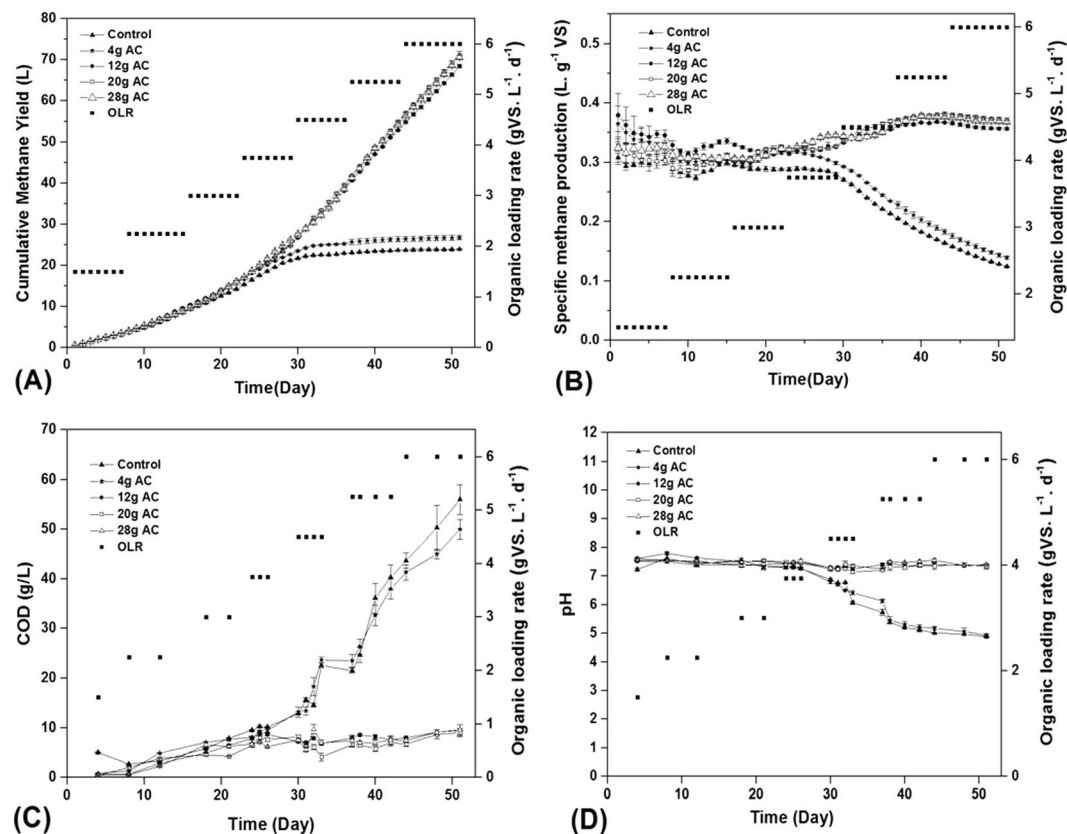


**Figure 1.** Effect of different dosages of AC on (A) Cumulative methane yield, (B) Specific methane production, (C) COD concentration and (D) pH.

Enhancing AD by the addition of conductive carbon materials in digesters to resist high OLRs has been recently reported<sup>8</sup>. Further studies showed that direct interspecies electron transfer (DIET) has been considered as an alternative to IHT for syntrophic metabolism<sup>9</sup>. This process can be explained as the mechanism of direct electron transfer from the bacteria to the electron-accepting methanogens via biological electrical connections, e.g. electrically conductive pili<sup>10</sup> and outer surface c-type cytochromes<sup>11</sup>. However, most of these studies have been conducted to explore only the potential mechanisms using simple substrates<sup>9</sup> or pure cultures<sup>10</sup> due to the complexity of the degradation process of complex organic substrates in AD process<sup>12</sup>, thus limiting the exploration of metabolic mechanism. For FW, in addition to syntrophic metabolism of AD intermediate products via IHT or DIET by syntrophic bacteria, hydrolyzing and fermenting process via other bacteria also plays an important role in AD process<sup>13</sup>. For example, the hydrolysis and acidogenesis of lipids is considered as a critical limiting step for AD of FW due to its bio-refractory and hydrophobic property<sup>14,15</sup>. Therefore, syntrophic metabolism is unlikely to work effectively unless hydrolysis and acidogenesis function well. However, the potential microbial networks and metabolic pathways at the whole community level have yet to be investigated, especially for AD of FW.

Based on the above consideration, adding AC in AD system was investigated for FW treatment and methane production. Deep insight into the effects of AC on the interactive relationship in a broad profile of microbial networks including hydrolyzing and fermenting bacteria, syntrophic bacteria, and methanogens was conducted by the metagenomic shotgun sequencing using high-throughput sequencing technology, which typically generates millions to billions of reads for the metagenomic DNA extracted from sludge samples of AD reactors. In addition, the effects of AC on the syntrophic mechanism and metabolic pathway of all microbes were explored by a method of metabolic pathway analysis that provided systematic information about gene function, protein function and enzymatic reaction based on the database of Kyoto Encyclopedia of Genes and Genomes. To the best of our knowledge, this is the first study to conduct multi-analysis regarding the taxonomic resolution of microbial communities and metabolic pathway of anaerobic microbes as well as association analysis of microbial network in AD process assisted by the addition of AC.

## Results and Discussion

**Effect of AC addition on methane production in AD of FW.** The effect of AC addition on methane production was investigated in five AD reactors operated in parallel: four AC enhanced AD reactors with the addition of different content of AC: 4g, 12g, 20g, and 28g and control AD reactors without the addition of AC. Cumulative methane yield (CMY) (Fig. 1A), specific methane production (SMP) (Fig. 1B), COD (Fig. 1C), and pH (Fig. 1D) were monitored at increasing OLR from 1.5 to 6 g VS·L<sup>-1</sup>·d<sup>-1</sup>.

In the initial 22 days of OLR up to  $3 \text{ g VS} \cdot \text{L}^{-1} \cdot \text{d}^{-1}$ , the average CMY and SMP in the five AD reactors were increased to  $15.6 \text{ L}$  and  $0.32 \text{ L} \cdot \text{g}^{-1} \text{ VS}$ , respectively, and all reactors operated stably with an average effluent pH of 7.4. Differences among the five AD reactors were hardly significant due to the low OLR. When the OLR was increased to  $6 \text{ g VS} \cdot \text{L}^{-1} \cdot \text{d}^{-1}$ , the CMY in AD reactors with the addition of AC greater than or equal to  $12 \text{ g}$  was maintained between  $68.5 \text{ L}$  and  $71.2 \text{ L}$  and SMP was kept between  $0.36 \text{ L} \cdot \text{g}^{-1} \text{ VS}$  and  $0.37 \text{ L} \cdot \text{g}^{-1} \text{ VS}$  with an average effluent pH of 7.3. The CMY was only  $24.2 \text{ L}$  and  $22.3 \text{ L}$  in the AD reactor with the addition of  $4 \text{ g}$  AC and control reactor, respectively, and the SMP had dropped to  $0.14 \text{ L} \cdot \text{g}^{-1} \text{ VS}$  and  $0.12 \text{ L} \cdot \text{g}^{-1} \text{ VS}$ , respectively, which might be caused by the high COD concentration of  $50$  to  $56 \text{ g} \cdot \text{L}^{-1}$  and low pH of  $5$  to  $6$ . These results indicate that  $12 \text{ g}$  AC is the optimal additive amount to tolerate high FW loading rates and promote methane production as increase in AC dosage cannot further improve AMY and SMP significantly, while AC dosage lower than  $12 \text{ g}$  has not positive effect on the enhancement of AD performance for methane production. This phenomenon can be explained by the abundance of archaea which comprise the majority of methanogens in AD reactors. From Fig. S1, 16S rRNA gene copy numbers of archaea in the sludge samples of AD reactors with  $12 \text{ g}$  AC was  $2.93 \times 10^6$  copies/ $\mu\text{L}$  - DNA, significantly higher than that of  $5.29 \times 10^5$  copies/ $\mu\text{L}$  - DNA in the AD reactors with  $4 \text{ g}$  AC. However, 16S rRNA gene copy numbers of archaea in AD reactors with  $20 \text{ g}$  AC and  $24 \text{ g}$  AC were only  $3.16 \times 10^6$  copies/ $\mu\text{L}$  - DNA and  $3.09 \times 10^6$  copies/ $\mu\text{L}$  - DNA, respectively, presenting no significant difference as compared with the AD reactors with  $12 \text{ g}$  AC.

AC is an amorphous, carbonaceous material exhibiting relatively high porosity, large surface area, and strong adsorption capability. Therefore, the surface of AC in the four AD reactors could provide an excellent environment for colonization by anaerobes, especially for methanogens, which likely helped the reactor operate stably. Too low amount of AC might reduce the amount of active sites of AC<sup>16</sup> and affect the enrichment of methanogens in the AD reactor<sup>16</sup>, a possible reason to explain the poor performance of the AD reactor with the addition of  $4 \text{ g}$  AC. However, excessive dosage of AC also cannot further enhance the enrichment of methanogens and improve reactor performance.

**Microbial community composition.** After 51 days of operation, the whole microbial community in the sludge samples of seed sludge, control reactor without AC (A1), and the AD reactor with the addition of  $12 \text{ g}$  AC (A2) were analyzed by metagenomic shotgun sequencing. Multiple species taxonomy analysis showed that bacterial and archaeal populations are dominant microbial communities, accounting for over 97% of total microbial populations (Fig. 2A,B). The remaining populations are *Metazoa*, Unclassified Viruses, Fungi, Viridiplantae, and *Plasmodium\_chabaudi*, revealing just a tiny fraction of the whole microbial communities. Hierarchical cluster analysis (Fig. S2) showed that the microbial community in seed sludge and A2 was classified to one cluster. This cluster was separated from A1, suggesting that the microbial community structure in A1 significantly changed without the addition of AC.

Error bar graphs of difference comparison in Fig. S3 further indicated that the difference of microbial communities between A2 and A1 and seed sludge was mainly attributed to the difference between proportions ( $p < 0.05$ ) of *Proteobacteria*, *Bacteroidetes*, and *Euryarchaeota*. *Proteobacteria* and *Bacteroidetes* include fermenting, acetogenic and syntrophic bacteria that can ferment organic compounds and degrade VFA<sup>17</sup>. As shown in the outer ring of cyclic phylogenetic trees in Fig. 2C,D, two dominant genera (*Smithella*, *Desulfobulbus*) under *Proteobacteria* and two dominant genera (*Flavobacterium* and *Lentimicrobium*) under *Bacteroidetes* in bacterial community were selectively enriched in A2 due to the addition of AC. The relative abundance of *Proteobacteria* in A2 were 16% of total microbial communities while it was only 5% in A1. *Desulfobulbus*, found with the ability of reducing sulfate to hydrogen sulfide, is also involved in the production of propionate and acetate via fermenting complex organic compounds<sup>18</sup>. *Smithella* was the typical syntrophic VFA oxidizing bacteria known to degrade butyrate and/or propionate to acetate with the production of  $\text{H}_2$ . This genera usually has syntrophic relationship with  $\text{H}_2$ -utilizing methanogens via IHT. Most of genera in *Bacteroidetes* are hydrolyzing and fermenting bacteria<sup>19</sup>, such as dominant genera *Flavobacterium* and *Lentimicrobiu*, as well as other genera such as *Bacteroidetes* and *Alistipes*. These genera are involved in VFA,  $\text{CO}_2$  and  $\text{H}_2$  generation, through carbohydrates, lipids and proteins fermentation producing enzymes for polysaccharides' and proteoglycans' cleavage<sup>19,20</sup>.

*Euryarchaeota* comprise the majority of methanogens in AD reactors. From Fig. 2A,B, over 93% of anaerobes in phylum *Euryarchaeota* belong to methanogens except *Thermoplasmata*, *Thermococcales*, and *Halobacteria*. The relative abundance of *Euryarchaeota* in A2 is 15% of total microbial communities, significantly higher than the 4% in seed sludge and 3% in A1. These results indicated that the addition of AC in A2 helped to enrich methanogens, playing a crucial role in improving methane yield during AD process. On the basis of metabolic pathway, methanogens can be categorized into aceticlastic methanogens and hydrogen-utilizing methanogens. As shown in the outer ring of cyclic phylogenetic trees in Fig. 2C,D, four dominant methanogenic archaea (A, B, C, D), three hydrogenotrophic methanogens (*Methanoregula*, *Methanolinea*, *Methanoculleus*), and one aceticlastic methanogen (*Methanosaeta*) were only enriched in A2. Even though A1 also has 3% of *Euryarchaeota*, the relative abundance of each genera is lower than 1% of total microbial communities. In the sludge samples of A2, *Methanosaeta* accounted for 5% of total microbial communities. As is known, *Methanosaeta* is capable of directly accepting electron from the reduction of  $\text{CO}_2$  to produce  $\text{CH}_4$  through participating DIET<sup>10</sup>. However, DIET has only been reported to occur in defined co-cultures of *Geobacter Metallireducens* and *Geobacter sulfurreducens* or *Geobacter* species and acetoclastic methanogens<sup>10,21</sup>. *Geobacter* is included in *Proteobacteria*. As shown in Fig. S4, the relative abundance of *Geobacter* genera in A2 was 0.8% of bacterial communities, much higher than the 0.08% in A1 and 0.3% in seed sludge, respectively. *Geobacter metallireducens* and *Geobacter sulfurreducens* are two dominant *Geobacter* species in A2 accounting for 25% of total *Geobacter* species. Together with the increase of *Methanosaeta* genera and *Geobacter* genera, the potential DIET between *Geobacter* and *Methanosaeta* might be established to improve the syntrophic metabolism of AD intermediate products e.g. propionate, butyrate, and ethanol. Therefore, the contribution of DIET on AD of FW in A2 might be enhanced via the addition of AC.

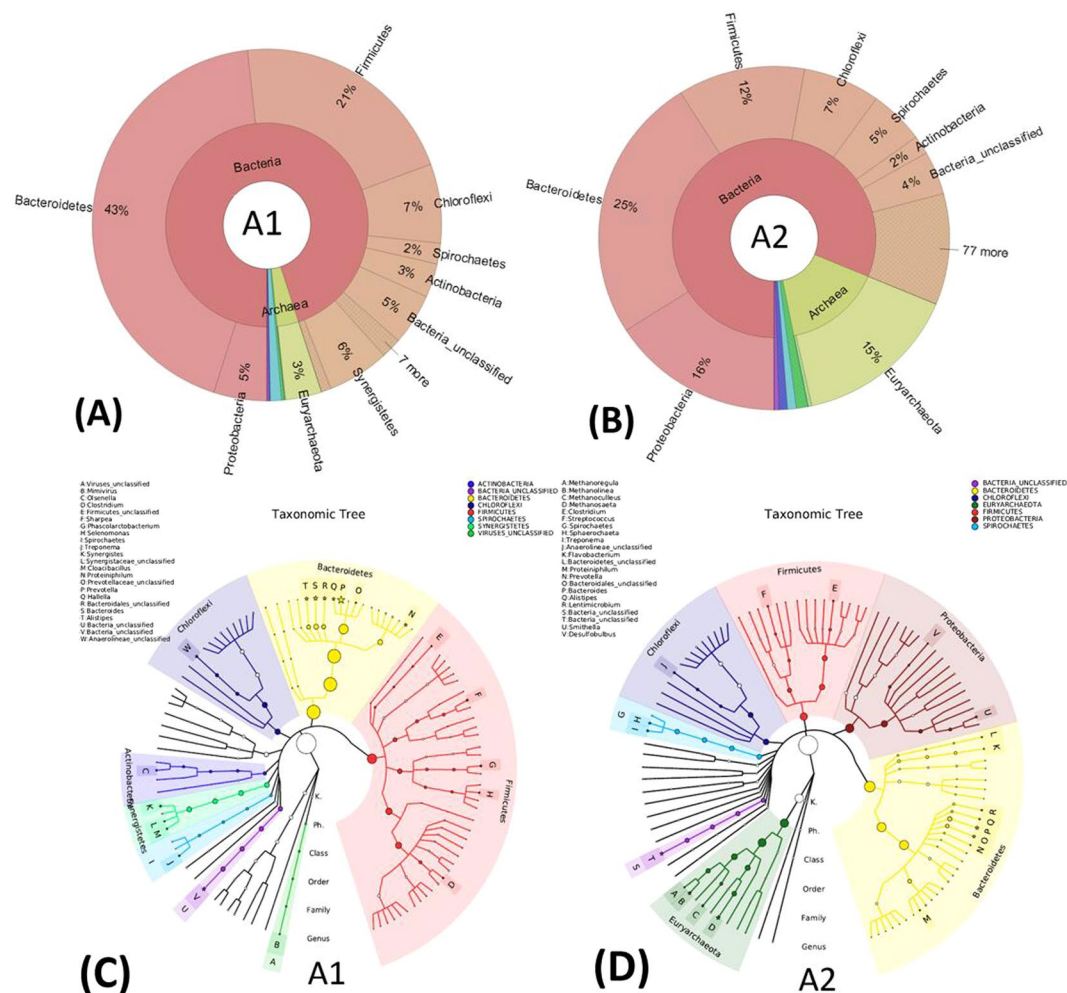


**Figure 2.** Schematic diagram of multi-level species taxonomy of the whole AD microbial community in the sludge samples of A1 (A) and A2 (B) after 51 days of operation. Microbial community compositions from the interior to external circle were identified at domain and phylum level by analysing merged paired-end based 16S rRNA genes. Phylogenetic and taxonomy trees of dominant AD microbial communities in reactor A1 (C) and A2 (D) according to GraPhlAn analysis. The top one hundred genus were selected to construct phylogenetic trees, and the corresponding phyla of top twenty genus (marked with asterisk) was marked in different color. The size of circles and asterisks represent the different relative abundance of microbial populations.

Furthermore, the dominant hydrogenotrophic methanogens, *Methanoregula*, *Methanolinea* and *Methanoculleus*, accounted for 41% of archaeal communities. The enrichment of hydrogenotrophic methanogens play a major role in keeping a low  $H_2$  pressure through reduction of  $CO_2/H_2$  to  $CH_4$  and has been found to be of importance for syntrophic metabolism of VFA to acetate by syntrophic oxidizing bacteria<sup>22</sup>.

**Microbial network and co-network.** The AD process generally requires multiple groups of microorganisms working together to convert organic substrates to methane. Therefore, to investigate a thorough microbial network in relation to the whole microbial community changes, understanding the relationship among different microorganisms is very important. In particular, analyzing the impact of AC on the microbial communities is crucial. As shown in Fig. 3A, a microbial co-network was constructed to present correlations among all microorganisms in A1, A2, and seed sludge. The area of all pie charts is similar except the pie of the “Other” is composed by several non-dominant microorganisms, suggesting that the difference of relative abundance of every microbial genera is hardly significant. This result might be partially attributed to the complexity of the substrate and degradation process that usually requires the joint action of multiple genera, as compared with simple substrate such as acetate that might only need a limiting amount of genera. The larger area of pie “Other” indicated that the function of some non-dominant microorganisms is also indispensable even though dominant microorganisms usually play a major role in AD process. The red line and green line respected the positive and negative correlations among different genera, respectively. Positive correlations usually contain cross-feeding, co-aggregation, co-colonization and niche overlap<sup>23</sup>, which are favorable for the syntrophic metabolism of AD intermediates among various genera. In AD conditions, negative correlations usually arose from competition for substrates and differential niche adaptation. The distribution of most genera is intensive except the genera locating at the external



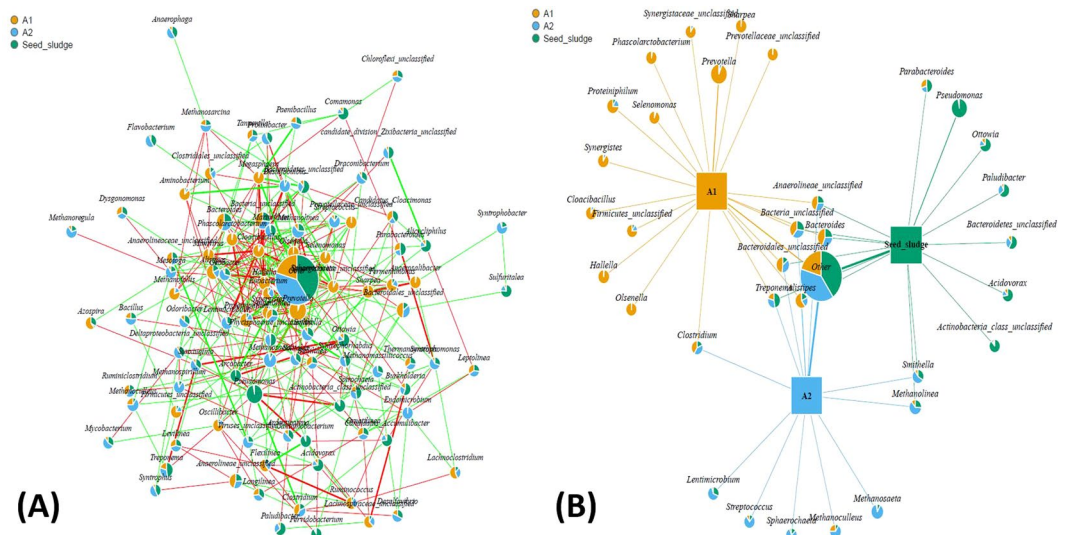


**Figure 3.** (A) The microbial co-network revealing intense interaction between different genus in all the sludge samples of reactor A1, A2 and seed sludge. Pie charts indicate the relative abundance of each genus. The red line represent the positive associations, while the green line represent the negative associations. (B) The microbial network indicating the shared and unique dominant genus among the seed sludge, reactor A1, and A2.

border, indicating that some genera has little relationship with AD process such as *Viruses\_unclassified*, *Azospira* and *Mesotoga* etc. while some genera are inseparable from AD process e.g. *Bacteroides* and *Methanosaeta*.

To further investigate the effects of AC on the interaction between different genera, a thorough microbial network among A1, A2 and seed sludge was constructed with dominant microbial populations that has significant difference ( $P < 0.05$ ) among each genera (Fig. 3B). This microbial network revealed topological features observed in complex systems, forming shared correlations and specific correlations. The main shared correlations is attributed to the same microorganisms existing within both A1 and A2 reactors, and within seed sludge e.g. *Bacteroides*, *Treponemalisticipes*, *Anaerolineae\_unclassified*, and others. These genera are involved in fermenting complex organic compounds to simple substrates such as VFA,  $\text{CO}_2$  and  $\text{H}_2$ . One possible explanation for the aggregation of these genera in the shared area is that hydrolysis and fermentation are the first steps in AD process via the action of hydrolyzing and fermenting bacteria that can survive against variable environment. However, the addition of AC in A2 changed the AD environment and reshaped the microbial network by forming some specific correlations that were attributed to the specific genera which only survive in A2 e.g. *Lentimicrobium*, *Streptococcus*, *Sphaerochaeta*, *Methanoculleus*, and *methanosaeta*. *Methanoculleus* and *Methanosaeta* are classified as hydrogenotrophic methanogen and acetoclastic methanogen, respectively. *Lentimicrobium*, *Streptococcus* and *Sphaerochaeta* are strictly fermentative bacteria which produce VFA, ethanol,  $\text{H}_2/\text{CO}_2$  by fermenting complex organics.

**Metabolic pathways of microbial communities.** To understand and exploit the impact of AC on microbial metabolism, the analysis of metabolic pathways of microbial communities was conducted. The predictive functional profiling of the microbial communities in A1 and A2 was shown in Fig. S5. All the metabolic functions were classified to Metabolism, Environmental\_Information\_Processing, Genetic\_information\_Processing, Cellular\_Processes, Human\_Diseases, and Organismal\_Systems, of which Metabolism was the most dominant category that included several metabolic pathways e.g. Carbohydrate Metabolism, Amino Acid\_Metabolism, Lipid Metabolism, Energy Metabolism, and Others. These metabolic pathways in Metabolism denotes the various biochemical processes responsible for the breakdown and mineralization of carbohydrate, proteins, and lipids in FW and bioenergy production. However, the differences of metabolic pathways between A1 and A2 were hardly significant except those of Energy Metabolism and Lipid Metabolism. Both of them were improved by 2% and 1%, respectively, in relative abundance of whole genome, due to the addition of AC in A2. To further verify the metabolic functions of microbial communities, analysis of gene functional classification were also conducted through comparing protein sequence with another database of COG (<https://www.ncbi.nlm.nih.gov/COG/>). As shown in Fig. S11, the gene numbers of Energy production and Lipid transport and metabolism in A2 were 15030 and 5395, respectively, while it were only 13863 and 4825 in A1, respectively. The enhancement of Energy Metabolism was mainly attributed to the pathway of Methane Metabolism (Ko00680) (Fig. 4), in which methanogens obtain energy for growth by converting simple substrates to methane during AD process (Fig. S6A). This might be a possible biological reason for the higher methane yield in A2.

Lipid Metabolism refers to the degradation of lipids. The improvement of Lipid Metabolism was ascribed to the pathway of Fatty Acids Degradation, in which hydrolyzing and fermenting bacteria converted long-chain fatty acids and glycerolipid to small molecule fatty acids via the action of several functional enzymes (Fig. S6B). The degradation of lipids is still considered to be the limiting step for AD of FW because of the bio-refractory compounds contained in lipids that mainly include fats and edible oil<sup>14</sup>. Moreover, the hydrophobic feature of



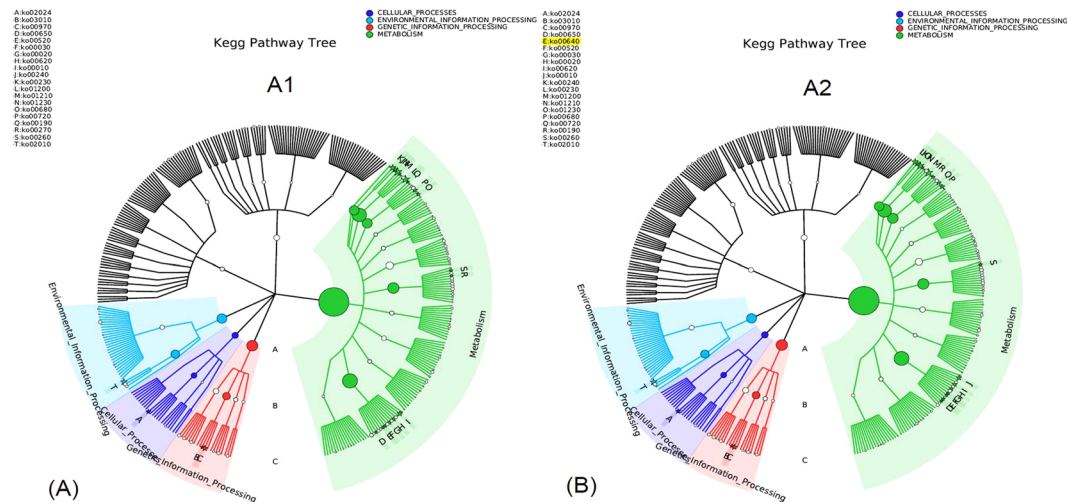


**Figure 5.** KEGG pathway trees represent the dominant metabolic pathways during AD process in reactor A1 and A2. Asterisks in the outer ring indicate the dominant metabolic pathways of reactor A1, A2. (A) reactor A1; (B) reactor A2.

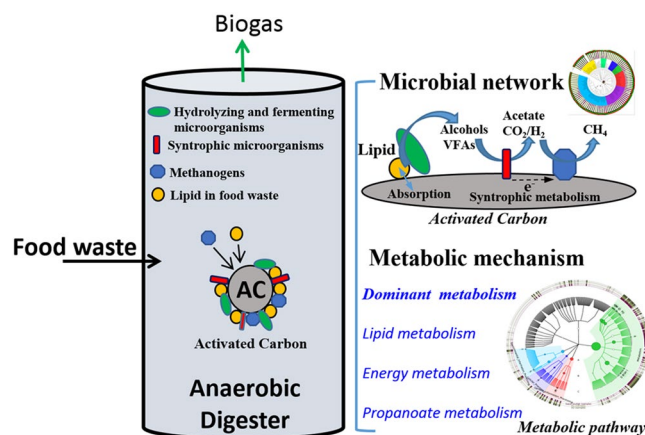


**Figure 6.** Conceptual graph of microbial network and dominant metabolic pathways of microbial communities in anaerobic digesters for food waste by incorporating AC.

further evidence of metabolic pathway analysis supported this speculation, since AC created a specific metabolic pathway of propanoate metabolism that accelerated the syntrophic metabolism of propionate. These findings demonstrate through investigating the 16S rRNA of the microbial community that the changes in microbial association network and biometabolic pathways explain how AC enhances AD of food waste.

## Conclusions

In this work, the use of AC in an anaerobic digestion system for food waste was explored. Using bioinformatics analysis, taxonomic trees and the KEGG Orthologs database, changes in microbial networks and biometabolic pathways were tracked.

- (1) 12 g AC in the reactor is the optimal additive amount to tolerate high FW loading rates.
- (2) Adding AC in wet AD system could enhance the metabolism of lipids in FW and facilitate archaea colonization, and subsequently accelerate the degradation rate of FW and methane production.
- (3) AC enhanced the biometabolic pathways of methane metabolism and lipid metabolism.
- (4) The addition of AC in AD process helped to construct an effective microbial network and accelerate the syntrophic metabolism. A specific metabolic pathway of propanoate metabolism was discovered by the addition of AC.

## Materials and Methods

**Inocula and substrates.** The seed sludge was collected from a large-scale anaerobic digester at Ulu Pandan Water Reclamation Plant in Singapore. The ratio of volatile suspended sludge (VS) to total suspended sludge (TS)



Sample	Total reads	No. of contigs	N50	Max Len	Total Len	Average Len	GC content
A1	76406684	500699	1327	410518	455780585	910.29	50.64%
A2	52543088	421867	1781	286352	465262942	1102.87	51.16%
Seed sludge	62331322	582851	1237	153117	547000062	938.49	55.27%

**Table 1.** The number of reads used for the analysis and the basic sequencing statistics of contigs.

was 0.65 with an initial TS of 13.2 g/L. FW was obtained from a canteen of the National University of Singapore, which mainly consisted of rice, noodles, meat, vegetables, and condiments. After removing any bones and non-biodegradable waste like plastic bags, FW was homogenized by a blender and then stored in a  $-20^{\circ}\text{C}$  freezer. The detailed characteristics of FW are listed in Table S1.

**Reactor specification and operation.** Two bench-scale experiments were conducted. First, four glass experimental anaerobic digesters were operated for FW treatment with the addition of different content of powdered AC (200 mesh): 4 g, 12 g, 20 g, and 28 g. The working volume of each digester was 0.8 L. Control digester is same to the experimental digesters but without the addition of powdered AC. The pore volume and surface area of powdered AC were 0.30 cc/g and 385 m<sup>2</sup>/g, respectively. After being seeded with seed sludge, these five anaerobic digesters were operated for AD of FW in a semi-continuous mode (feeding every day) with a gradual increase in the organic loading rate (OLR). All reactors were operated at 35 °C in parallel. The sludge retention time was 30 d. All the experiments were conducted in triplicate.

After getting the optimum dosage of AC for AD of FW, two glass experimental anaerobic digesters were operated for the treatment of edible oil of food waste with the addition of 12 g AC (hereafter referred to as ACR). Control digester is same to the experimental digesters but without the addition of powdered AC (hereafter referred to as CR). Edible oil was used as sole substrate. The working volume of each digester was 0.8 L. All reactors were operated at 35 °C in parallel. The sludge retention time was 30 d. All the experiments were conducted in triplicate.

**Analytical methods.** COD were determined using HACH color meter (DR900, USA) according to the manufacturer's instructions. The pH was recorded using a pH analyzer (Agilent 3200 M, USA). TS and VS were determined based on the weighing method after being dried at 103–105 °C and burnt to ash at 550 °C. The CH<sub>4</sub> production was determined using a gas chromatograph (Clarus 580 Arnel, PerkinElmer, USA) equipped with a thermal conductivity detector. C, N, S and H elemental analyses in FW were determined using the vario MICRO cube (Elementar, HANAU, Germany). Metals elemental analyses were conducted using an inductively coupled plasma (ICP) – optical emission spectrometer (Perkin Elmer Optima 5300 V, USA). BET surface area and pore volume of activated carbons were measured by N<sub>2</sub> adsorption measurement using a Quantachrome Autosorb-6B. Real-time PCR was used to quantify total archaea according to the methods described by Zhang *et al.*<sup>24</sup>.

**Metagenomic shotgun sequencing and metabolic pathways analysis.** Sequencing of metagenomic DNA was conducted by Illumina HiSeq™ sequencer (Illumina Inc., USA). The analytical methods refer to the reference<sup>25</sup> that includes DNA extraction, DNA library construction and sequencing, screening of effective reads, assembling of high-quality reads of DNA samples, Gene taxonomic assignment, Gene functional classification, and other related analyses.

Briefly, the metagenomic DNA of the sample was extracted using an extraction kit (MOBIO Laboratories, Inc. Carlsbad, USA) according to the manufacturer's instructions. The purity of the extracted DNA was checked by determining its absorbance at 260 nm and 280 nm, and we measured the concentration of the DNA using a Qubit 2.0 (Life, USA). To obtain the effective and clean sequencing data, raw sequencing results were processed by Trimmomatic<sup>26</sup> as follows: (1) trimmed adaptor sequences of reads; (2) removed sequences containing ambiguities ("Ns"); (3) removed reads shorter than 35 nt. (4) removed low - quality sequences i.e. a sequencing quality value lower than 20; (5) removed sequences with the quality of the tail less than 20 bases by sliding window protocol. Effective reads were assembled by IDBA\_UD software according to the relationships between reads and overlap to obtain contigs that was further translated into protein sequences<sup>27</sup>. The number of total reads and the basic sequencing statistics of contigs was shown in Table 1. Subsequently, taxonomy was assigned by MetaPhlan2 software through blasting marker genes with effective reads<sup>28</sup>. Analysis of metabolic pathways and gene functional classification were conducted by DIAMOND<sup>29</sup> and HUMAnN<sup>30</sup> through comparing protein sequence with database of Kyoto Encyclopedia of Genes and Genomes (KEGG)<sup>31–35</sup>. Configuration diagram of multiple species/functions including was constructed using Krona<sup>36</sup> and GraPhlAn<sup>37</sup>. The construction of clustering tree was made according to the hierarchical clustering analysis based on the unweighted pair group method with arithmetic mean. Based on the results of taxonomy, analysis of variance of species was done by STAMP with a screening condition of P value lower than 0.05<sup>38</sup>. Microbial network and co-network were analyzed by QIIME<sup>38</sup> and SPARCC with dominant species (relative abundance  $\geq 1\%$ ), respectively.

## References

1. Thyberg, K. L., Tonjes, D. J. & Gurevitch, J. Quantification of Food Waste Disposal in the United States: A Meta-Analysis. *Environmental Science & Technology* **49**(24), 13946–13953 (2015).
2. Zhang, J. X. *et al.* Three-stage anaerobic co-digestion of food waste and horse manure. *Scientific Reports* **7**, 1269 (2017).
3. Yan, B. H., Selvam, A. & Wong, J. W. C. Innovative method for increased methane recovery from two-phase anaerobic digestion of food waste through reutilization of acidogenic off-gas in methanogenic reactor. *Bioresour. Technol.* **217**, 3–9 (2016).



4. Zhang, C., Su, H., Baeyens, J. & Tan, T. Reviewing the anaerobic digestion of food waste for biogas production. *Renewable and Sustainable Energy Reviews* **38**, 383–392 (2014).
5. Hartmann, H. & Ahring, B. K. Anaerobic digestion of the organic fraction of municipal solid waste: Influence of co-digestion with manure. *Water Research* **39**(8), 1543–1552 (2005).
6. Sieber, J. R., McInerney, M. J. & Gunsalus, R. P. Genomic Insights into Syntrophy: The Paradigm for Anaerobic Metabolic Cooperation. In *Annual Review of Microbiology*, (Gottesman, S., Harwood, C. S. & Schneewind, O. Eds), Vol. 66, pp 429–452 (2012).
7. Stams, A. J. M. & Plugge, C. M. Electron transfer in syntrophic communities of anaerobic bacteria and archaea. *Nature Reviews Microbiology* **7**(8), 568–577 (2009).
8. Zhao, Z. Q., Zhang, Y. B., Woodard, T. L., Nevin, K. P. & Lovley, D. R. Enhancing syntrophic metabolism in up-flow anaerobic sludge blanket reactors with conductive carbon materials. *Bioresource Technology* **191**, 140–145 (2015).
9. Zhao, Z. *et al.* Communities stimulated with ethanol to perform direct interspecies electron transfer for syntrophic metabolism of propionate and butyrate. *Water Research* **102**, 475–484 (2016).
10. Rotaru, A. E. *et al.* A new model for electron flow during anaerobic digestion: direct interspecies electron transfer to Methanosaeta for the reduction of carbon dioxide to methane. *Energy & Environmental Science* **7**(1), 408–415 (2014).
11. Summers, Z. M. *et al.* Direct Exchange of Electrons Within Aggregates of an Evolved Syntrophic Coculture of Anaerobic Bacteria. *Science* **330**(6009), 1413–1415 (2010).
12. Lei, Y. Q. *et al.* Stimulation of methanogenesis in anaerobic digesters treating leachate from a municipal solid waste incineration plant with carbon cloth. *Bioresource Technology* **222**, 270–276 (2016).
13. Speece, R. E. Anaerobic Biotechnology For Industrial Wastewater-Treatment. *Environmental Science & Technology* **17**(9), A416–A427 (1983).
14. Chen, Y., Cheng, J. J. & Creamer, K. S. Inhibition of anaerobic digestion process: A review. *Bioresource Technology* **99**(10), 4044–4064 (2008).
15. Cammarota, M. C., Teixeira, G. A. & Freire, D. M. G. Enzymatic pre-hydrolysis and anaerobic degradation of wastewaters with high fat contents. *Biotechnology Letters* **23**(19), 1591–1595 (2001).
16. Xu, S. *et al.* Comparing activated carbon of different particle sizes on enhancing methane generation in upflow anaerobic digester. *Bioresource Technology* **196**, 606–612 (2015).
17. Krakat, N., Schmidt, S. & Scherer, P. Potential impact of process parameters upon the bacterial diversity in the mesophilic anaerobic digestion of beet silage. *Bioresource Technology* **102**(10), 5692–5701 (2011).
18. Laanbroek, H. J., Abee, T. & Voogd, I. L. Alcohol Conversions By *Desulfobulbus-Propionicus* Lindhorst In The Presence And Absence Of Sulfate And Hydrogen. *Archives of Microbiology* **133**(3), 178–184 (1982).
19. Wirth, R. *et al.* Characterization of a biogas-producing microbial community by short-read next generation DNA sequencing. *Biotechnology for Biofuels* **5** (2012).
20. Yi, J., Dong, B., Jin, J. W. & Dai, X. H. Effect of Increasing Total Solids Contents on Anaerobic Digestion of Food Waste under Mesophilic Conditions: Performance and Microbial Characteristics Analysis. *Plos One* **9**(7) (2014).
21. Lovley, D. R. *et al.* Geobacter: The Microbe Electric's Physiology, Ecology, and Practical Applications. In *Advances in Microbial Physiology*, (Poole, R. K. Ed.) Vol. 59, pp 1–100 (2011).
22. Bassani, I., Kougias, P. G., Treu, L. & Angelidaki, I. Biogas Upgrading via Hydrogenotrophic Methanogenesis in Two-Stage Continuous Stirred Tank Reactors at Mesophilic and Thermophilic Conditions. *Environmental Science & Technology* **49**(20), 12585–12593 (2015).
23. Faust, K. & Raes, J. Microbial interactions: from networks to models. *Nature Reviews Microbiology* **10**(8), 538–550 (2012).
24. Zhang, J. X., Zhang, Y. B. & Quan, X. Bio-electrochemical enhancement of anaerobic reduction of nitrobenzene and its effects on microbial community. *Biochemical Engineering Journal* **94**, 85–91 (2015).
25. Qin, J. J. *et al.* A human gut microbial gene catalogue established by metagenomic sequencing. *Nature* **464**(7285), 59–U70 (2010).
26. Bolger, A. M., Lohse, M. & Usadel, B. Trimmomatic: a flexible trimmer for Illumina sequence data. *Bioinformatics* **30**(15), 2114–2120 (2014).
27. Peng, Y., Leung, H. C. M., Yiu, S. M. & Chin, F. Y. L. IDBA-UD: a de novo assembler for single-cell and metagenomic sequencing data with highly uneven depth. *Bioinformatics* **28**(11), 1420–1428 (2012).
28. Truong, D. T. *et al.* MetaPhlan2 for enhanced metagenomic taxonomic profiling. *Nature Methods* **12**(10), 902–903 (2015).
29. Buchfink, B., Xie, C. & Huson, D. H. Fast and sensitive protein alignment using DIAMOND. *Nature Methods* **12**(1), 59–60 (2015).
30. Abubucker, S. *et al.* Metabolic Reconstruction for Metagenomic Data and Its Application to the Human Microbiome. *Plos Computational Biology*, **8**(6) (2012).
31. Kanehisa, M., Sato, Y. & Morishima, K. BlastKOALA and GhostKOALA: KEGG Tools for Functional Characterization of Genome and Metagenome Sequences. *Journal of Molecular Biology* **428**(4), 726–731 (2016).
32. Kanehisa, M., Tanabe, M., Sato, Y. & Morishima, K. KEGG: new perspectives on genomes, pathways, diseases and drugs. *Nucleic Acids Research* **45**, D353–D361 (2017).
33. Kanehisa, M., Sato, Y., Kawashima, M., Furumichi, M. & Tanabe, M. KEGG as a reference resource for gene and protein annotation. *Nucleic Acids Research* **44**, D457–D462 (2016).
34. Kanehisa, M. & Goto, S. KEGG: Kyoto Encyclopedia of Genes and Genomes. *Nucleic Acids Res.* **28**, 27–30 (2000).
35. Kanehisa, M. “*Post-genome Informatics*”, (Oxford University Press, 2000).
36. Ondov, B. D., Bergman, N. H. & Phillippy, A. M. Interactive metagenomic visualization in a Web browser. *Bmc Bioinformatics* **12** (2011).
37. Asnicar, F., Weingart, G., Tickle, T. L., Huttenhower, C. & Segata, N. Compact graphical representation of phylogenetic data and metadata with GraPhlAn. *PeerJ* **3** (2015).
38. Langille, M. G. I. *et al.* Predictive functional profiling of microbial communities using 16S rRNA marker gene sequences. *Nature Biotechnology* **31**(9), 814–+ (2013).

## Acknowledgements

This research/project is supported by the National Research Foundation, Prime Minister's Office, Singapore under its Campus for Research Excellence and Technological Enterprise (CREATE) programme.

## Author Contributions

J.X.Z., K.C.L. and Y.W.T. supervised the experiments. J.X.Z. wrote the manuscript. J.X.Z., L.W.M. and L.Z. conducted most of the experiments; J.X.Z., K.C.L. and Y.W.T. performed the data analysis and discussion. All authors reviewed the manuscript.

## Additional Information

**Supplementary information** accompanies this paper at doi:10.1038/s41598-017-11826-5

**Competing Interests:** The authors declare that they have no competing interests.

**Publisher's note:** Springer Nature remains neutral with regard to jurisdictional claims in published maps and institutional affiliations.



**Open Access** This article is licensed under a Creative Commons Attribution 4.0 International License, which permits use, sharing, adaptation, distribution and reproduction in any medium or format, as long as you give appropriate credit to the original author(s) and the source, provide a link to the Creative Commons license, and indicate if changes were made. The images or other third party material in this article are included in the article's Creative Commons license, unless indicated otherwise in a credit line to the material. If material is not included in the article's Creative Commons license and your intended use is not permitted by statutory regulation or exceeds the permitted use, you will need to obtain permission directly from the copyright holder. To view a copy of this license, visit <http://creativecommons.org/licenses/by/4.0/>.

© The Author(s) 2017